Nanofluid slip flow over a stretching cylinder with Schmidt and Péclet number effects

Md Faisal Md Basir, M. J. Uddin, A. I. Md. Ismail, and O. Anwar Bég

Citation: AIP Advances **6**, 055316 (2016); doi: 10.1063/1.4951675
View online: http://dx.doi.org/10.1063/1.4951675
View Table of Contents: http://aip.scitation.org/toc/adv/6/5
Published by the American Institute of Physics

Nanofluid slip flow over a stretching cylinder with Schmidt and Péclet number effects

Md Faisal Md Basir,[1,a] M. J. Uddin,[2] A. I. Md. Ismail,[1] and O. Anwar Bég[3]
[1]*School of Mathematical Sciences, Universiti Sains Malaysia, 11800, Penang, Malaysia*
[2]*American International University-Bangladesh, Banani, Dhaka 1213, Bangladesh*
[3]*Spray Research Group, School of Computing, Science and Engineering, Newton Bldg, University of Salford, Manchester, M54WT, England, UK*

(Received 20 February 2016; accepted 3 May 2016; published online 18 May 2016)

A mathematical model is presented for three-dimensional unsteady boundary layer slip flow of Newtonian nanofluids containing gyrotactic microorganisms over a stretching cylinder. Both hydrodynamic and thermal slips are included. By applying suitable similarity transformations, the governing equations are transformed into a set of nonlinear ordinary differential equations with appropriate boundary conditions. The transformed nonlinear ordinary differential boundary value problem is then solved using the Runge-Kutta-Fehlberg fourth-fifth order numerical method in **Maple 18** symbolic software. The effects of the controlling parameters on the dimensionless velocity, temperature, nanoparticle volume fractions and microorganism motile density functions have been illustrated graphically. Comparisons of the present paper with the existing published results indicate good agreement and supports the validity and the accuracy of our numerical computations. Increasing bioconvection Schmidt number is observed to depress motile micro-organism density function. Increasing thermal slip parameter leads to a decrease in temperature. Thermal slip also exerts a strong influence on nano-particle concentration. The flow is accelerated with positive unsteadiness parameter (accelerating cylinder) and temperature and micro-organism density function are also increased. However nano-particle concentration is reduced with positive unsteadiness parameter. Increasing hydrodynamic slip is observed to boost temperatures and micro-organism density whereas it decelerates the flow and reduces nano-particle concentrations. The study is relevant to nano-biopolymer manufacturing processes. [http://dx.doi.org/10.1063/1.4951675]

NOMENCLATURE

$\overline{a}$	radius (m)
a_0	constant (m)
b	velocity slip parameter $\left(b = \frac{2\,(N_1)_0\nu}{a_0}\right)$ $(-)$
c	thermal slip parameter $\left(c = \frac{2(D_1)_0}{a_0}\right)$ $(-)$
$\tilde{b}$	chemotaxis constant (m)
C	nanoparticles volume fraction $(-)$
$C_{f_{\bar{x}}}$	local skin friction coefficient $(-)$
c_p	specific heat at constant pressure $\left(\frac{J}{kg\,K}\right)$
C_∞	ambient nanoparticle volume fraction $(-)$
D_B	Brownian diffusion coefficient $\left(\frac{m^2}{s}\right)$
D_n	miroorganism diffusion coefficient $\left(\frac{m^2}{s}\right)$

[a]Corresponding author: Email - faisalbasir91@gmail.com

D_T thermophoretic diffusion coefficient $\left(\frac{m^2}{s}\right)$
D_1 variable thermal slip factor (m)
$(D_1)_0$ constant thermal slip factor (m)
$f(\eta)$ dimensionless stream function $(-)$
$\vec{j}$ vector flux of microorganism $\left(\frac{kg}{m^2 s}\right)$
k thermal conductivity $\left(\frac{W}{mK}\right)$
N_1 variable first order velocity slip factor $\left(\frac{s}{m}\right)$
$(N_1)_0$ constant first order velocity slip factor $\left(\frac{s}{m}\right)$
$Nn_{\bar{x}}$ local density number of motile microorganisms $(-)$
Nb Brownian motion parameter $\left(Nb = \frac{\tau D_B C_\infty}{\alpha}\right)$ $(-)$
Nt thermophoresis parameter $\left(Nt = \frac{\tau D_T (T_w - T_\infty)}{\alpha T_\infty}\right)$ $(-)$
$Nu_{\bar{x}}$ local Nusselt number $(-)$
n number of motile microorganism $(-)$
n_w wall motile microorganism $(-)$
Pe bioconvection Péclet number $\left(Pe = \frac{\tilde{b} W_c}{D_n}\right)$ $(-)$
P Pressure $\left(\frac{N}{m^2}\right)$
Pr Prandtl number $\left(\mathrm{Pr} = \frac{\upsilon}{\alpha}\right)$ $(-)$
q_m surface mass flux $\left(\frac{m}{s}\right)$
q_n surface motile microorganisms flux $\left(\frac{W}{m^2 K}\right)$
q_w surface heat flux $\left(\frac{W}{m^2}\right)$
$\overline{r}$ dimensional radial axis (m)
S unsteadiness parameter $(-)$
Sb bioconvection Schmidt number $\left(Sb = \frac{\upsilon}{D_n}\right)$ $(-)$
Sc Schmidt number $\left(Sc = \frac{\upsilon}{D_B}\right)$ $(-)$
$Sh_{\bar{x}}$ local Sherwood number (-)
$\overline{t}$ dimensional time (s)
T nanofluid temperature (K)
T_w surface temperature (K)
T_∞ ambient temperature (K)
$\overline{u}$ dimensional velocity components along the $\overline{r}-$ axis $\left(\frac{m}{s}\right)$
u dimensionless velocity component along the $\overline{r}-$ axis $(-)$
$\vec{\overline{v}}$ velocity vector $\left(\frac{m}{s}\right)$
$\overline{v}$ velocity components along the $\overline{y}-$ axis $\left(\frac{m}{s}\right)$
v dimensionless velocity component along the $y-$ axis $(-)$
$\overline{w}$ velocity components along the $\overline{z}-$ axis $\left(\frac{m}{s}\right)$
w dimensionless velocity component along the $z-$ axis $(-)$
W_c maximum cell (micro-organism) swimming speed $\left(\frac{m}{s}\right)$
$\overline{x}$ dimensional coordinate along the surface (m)
x dimensionless coordinate along the surface $(-)$
$\overline{y}$ coordinate normal to the surface (m)
y dimensionless coordinate normal to the surface$(-)$
$\overline{z}$ dimensional axial axis (m)
z dimensionless axial axis $(-)$

Greek letters

α effective thermal diffusivity $\left(\frac{m^2}{s}\right)$
β constant of the expansion/contraction strength $\left(\frac{1}{s}\right)$
η independent similarity variable $(-)$
$\theta(\eta)$ dimensionless temperature $(-)$
μ dynamic viscosity $\left(\frac{kg}{ms}\right)$
υ kinematic viscosity $\left(\frac{m^2}{s}\right)$

ρ	fluid density $\left(\frac{kg}{m^3}\right)$
$(\rho c)_f$	volumetric heat capacity of the fluid $\left(\frac{J}{m^3K}\right)$
$(\rho c)_p$	volumetric heat capacity of the nanoparticle material $\left(\frac{J}{m^3K}\right)$
τ	ratio of the effective heat capacity of the nanoparticle material to the fluid heat capacity $\left(\frac{(\rho c)_p}{(\rho c)_f}\right)$ (−)
τ_w	surface shear stress (−)
$\phi(\eta)$	dimensionless nanoparticles volume fraction (−)
$\chi(\eta)$	dimensionless number density of motile microorganism (−)

Subscripts

$(\ )'$	ordinary differentiation with respect to η
$(\ )_w$	condition at wall

I. INTRODUCTION

Studies on flows over stretching surfaces are important in manufacturing processes such as aerodynamic extrusion of plastic sheets, boundary layer liquid film condensation, paper production and glass blowing.[1] Stasiak et al.[2] have reported in detail on the influence of stretching on fluid mechanical properties of biopolymer cylinder coatings. Furthermore in Thomas and Yang[3] many applications are documented for stretching nano-bio-polymers on cylinders, sheets, wedges and other geometries to achieve modified properties. Stretching (or contracting) are therefore important technologies which are critical to the performance of polymer products from the macroscopic to the nanoscale. After the pioneering work of Khan and Pop[4] several researchers have studied stretching hydrodynamic flows with mass and heat transfer. Steady boundary layer flow due to a stretching surface in a quiescent viscous and incompressible fluid with the Oberbeck-Boussinesq approximation has been considered by Partha et al.[5] and Ishak et al.,[6] Bég et al.[7] (with magnetohydrodynamic and cross-diffusion effects) and Daskalakis.[8] Akl[9] quite recently investigated unsteady boundary layer flow due to a stretching cylinder with prescribed temperature and obtained the solution analytically. Bég et al.[10] studied stretching flow of a magnetic polymer using the homotopy analysis method.

A significant development in materials science and thermal engineering in the past two decades has been that of *nanofluids*. Nanofluids constitute a liquid suspension containing very fine particles (diameter less than 50 nm) in a base fluid such as water, oil, ethylene glycol etc.[11] Nanoparticles can be made from nitride ceramics (AlN, SiN), metals (Cu, Ag, Au) and semiconductors (SiC). The accumulation of nanoparticles into the base fluid can enhance the fluid flow and heat transfer proficiency of the liquids and increase the low thermal conductivity of the base fluid. This has implications in medical applications, power generation, micro-manufacturing, thermal therapy for cancer treatment, chemical and metallurgical sectors, microelectronics, aerospace and manufacturing.[12] Representative works on convective boundary layer flow and application of nanofluids were conducted by Buongiorno,[13] Das et al.,[14] Kakaç and Pramuanjaroenkij,[15] Saidur et al.[16] and Wen et al.[17] Further studies have been communicated by Mahian et al.,[18] Nield and Bejan,[19] Haddad et al.,[20] Sheremet and Pop[21] and many others. There are two types of model for nanofluids which have been commonly used by the researchers, namely Buongiorno's model[13] and the Tiwari-Das model.[22] According to Buongiorno, the velocity of the nanofluid is considered as the sum of the base fluid velocity and the relative/slip velocity. His model emphasizes the dominant mechanisms as Brownian diffusion and thermophoresis. In contrast to Buongiorno's model, the Tiwari-Das model[22] considers the solid volume fraction of the nanoparticles. The Buongiorno model[13] implies that the Brownian diffusion and thermophoresis are the most prominent parameters the characteristise nanofluid flows. Recently, work on convective boundary layer flow in nanofluids include Ghanbarpour et al.,[23] Li et al.,[24] Vanaki et al.,[25] Zhao et al.,[26] Serna,[27] Mohyud-Din[28] and others. Ferdows et al.[29] investigated radiative magnetohydrodynamic nano-polymer stretching flows. Uddin et al.[30] studied numerically the stretching fluid dynamics of magnetic nano-bio-polymers.

Bioconvection refers to a *macroscopic* convection motion of fluid affected by density gradients induced by hydrodynamic propulsion i.e. swimming, of motile microorganisms (see Kuznetsov[31]).

Adding microorganisms (such as algae and bacteria) to base fluids (e.g. water) creates the process of bioconvection which is directionally-orientated swimming typically towards an imposed or naturally present stimulus e.g. light, gravity, magnetic field and chemical concentration (oxygen). The density of the microorganism is inclined to be greater than that of the free stream fluid and this can cause an unstable density profile with subsequent upending of the fluid against gravity (see Raees et al.[32]). The base fluid has to be water for the majority of microorganisms to survive and be active and it is assumed nanoparticle suspension remains stable and do not agglomerate for a couple of weeks (see Anoop et al.[33]). For bioconvection to take place, the suspension must be dilute since nanoparticles would increase the suspension's viscosity and viscosity tends to dominates bioconvection instability (see Pedley[34]).

A recent innovation for microfluidic devices is to combine nanofluids with bioconvection phenomena (see Xu and Pop[35]). Aziz et al.[36] have studied theoretically the natural bio-convection boundary layer flow of nanofluids and verified that the bioconvection parameters influence mass, heat, and motile microorganism transport rates. Latiff et al.[37] studied unsteady forced bioconvection slip flow of a micropolar nanofluid from a stretching/shrinking sheet. Bioconvection may have also have a role to play in bio-microsystems for mass transport augmentation and microfluidic devices such as bacteria-powered micromixers (see Tham et al.[38]). Other significant applications of *nanofluid bioconvection* arise in the synthesis of novel pharmacological agents (drugs) as elaborated by Saranya and Radha[39] and earlier for nano-bio-gels as discussed by Oh et al.[40] Micro-organisms can be deployed strategically to enhance biodegradable polymeric nanomaterials and improve various desirable medical characteristics such as bioavailability, biocompatibility, encapsulation, DNA embedding in gene therapy, protein deliverability etc. The intelligent manufacture of bio-nano-polymers allows drugs to be developed which achieve a "controlled release" and this has been shown to increase therapeutic influence in patients. Examples of such bio-nano-polymers are poly (lactic-co-glycolic acid), polylactic acid, chitosan, gelatin, poly hydroxy alkaonates, poly caprolactone and poly alkyl cyanoacrylate.

To optimize the fabrication of bio-nano-materials, numerical and physico-mathematical simulation has an important role to play. This is a strong motivation for the present study in which the objective is to investigate the *effect of velocity slip, thermal slip and zero mass flux boundary conditions on time-dependent bioconvection nanofluid boundary layer flow from a horizontal cylinder*. The effects of selected biophysical and thermo-physical parameters on the dimensionless velocity, temperature, nanoparticle volume fraction, microorganism density function and furthermore on rate of heat transfer, the rate of nanoparticle volume fraction and the rate of motile microorganism density transfer rate are shown graphically and discussed. Validation of the present solutions which are obtained via MAPLE18 symbolic software is conducted with earlier studies.

II. BIOCONVECTION NANOFLUID MATHEMATICAL MODEL

Consider the unsteady forced bioconvection flow of a nanofluid that contains both nanoparticles and gyrotactic microorganisms over an infinite cylinder in contracting motion as shown in Fig. 1. The diameter of the cylinder is assumed to be a function of time with unsteady radius $\overline{a}\left(\bar{t}\right) = a_0\sqrt{1-\beta\,\bar{t}}$ where β the constant of the expansion/contraction strength, $\bar{t}$ is the time and a_0 is the positive constant.

The nanoparticles fraction on the ambient is assumed to obey the passively controlled model proposed by Kuznetsov and Nield[42], while the nanoparticles and temperature distribution on the ambient is assumed to be a constant C_∞, T_∞ respectively. It is worth mentioning that the micro-organisms can only survive in water. This indicates that the base fluid has to be water. Under these assumptions and the nanofluid model of Kuznetsov and Nield,[42] the relevant transport equations are the conservation of total mass, momentum, thermal energy, nanoparticle volume fraction and microorganisms concentration (density) which may be stated in vector form as follows: (see Xu and Pop[36])

$$\nabla\cdot\ \vec{\bar{v}} = 0, \tag{1}$$

$$\frac{\partial\vec{\bar{v}}}{\partial\bar{t}} + \left(\vec{\bar{v}}\ \cdot\ \nabla\right)\vec{\bar{v}} = -\frac{1}{\rho}\ \nabla\vec{P} + \upsilon\ \nabla^2\vec{\bar{v}}, \tag{2}$$

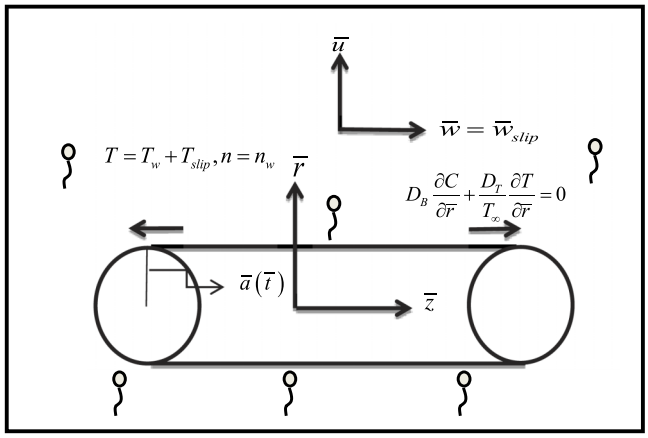

FIG. 1. The physical model and coordinate system (see Fang et al.[41]).

$$\frac{\partial T}{\partial \overline{t}} + \vec{\overline{v}} \cdot \nabla T = \alpha \nabla^2 T + \tau \left[D_B \nabla T \cdot \nabla C + \left(\frac{D_T}{T_\infty} \right) \nabla T \cdot \nabla T \right], \tag{3}$$

$$\frac{\partial C}{\partial \overline{t}} + \vec{\overline{v}} \cdot \nabla C = D_B \nabla^2 C + \tau \left[\left(\frac{D_T}{T_\infty} \right) \nabla^2 T \right], \tag{4}$$

$$\frac{\partial n}{\partial \overline{t}} + \nabla \cdot \vec{j} = 0, \tag{5}$$

where $\vec{\overline{v}} = (\overline{u}, \overline{v}, \overline{w})$ is the velocity vector of the nanofluid flow in the $\overline{x}-$direction, $\overline{y}-$direction and the $\overline{z}-$direction respectively, p is the pressure, T is the temperature, C is the nanoparticle volumetric fraction, n is the density of the motile microorganism, ρ is the nanofluid density, υ is the kinematic viscosity of the suspension of nanofluid and microorganisms, α is the thermal diffusivity of the nanofluid, $\tau = \frac{(\rho c)_p}{(\rho c)_f}$ is a parameter with $(\rho c)_p$ being heat capacity of the nanoparticle and $(\rho c)_f$ being the heat capacity of fluid, D_B is the Brownian diffusion coefficient, D_T is the thermophoretic diffusion coefficient, T_∞ is ambient temperature, $\vec{j}$ is the flux of microorganisms due to fluid convection, self-propelled swimming, *and diffusion,* which is defined by $\vec{j} = n \vec{\overline{v}} + n \hat{\vec{\overline{v}}} - D_n \nabla n$. Also $\hat{\vec{\overline{v}}} = \left(\frac{\tilde{b} W_c}{C_\infty} \right) \nabla C$ is the velocity vector relating to the cell swimming in nanofluids with D_n being the diffusivity of microorganisms, $\tilde{b}$ being the chemotaxis constant and Wc being the maximum cell swimming speed. In cylindrical polar coordinates, $\overline{r}$ and $\overline{z}$ are measured in the radial and axial directions, respectively, and based on the axisymmetric flow assumptions with boundary layer approximations and an order of magnitude analysis, neglecting azimuthal velocity component, Eqns. (1)–(5) can be written as: (see Zaimi et al.[43])

$$\frac{\partial \overline{u}}{\partial \overline{r}} + \frac{\overline{u}}{\overline{r}} + \frac{\partial \overline{w}}{\partial \overline{z}} = 0, \tag{6}$$

$$\frac{\partial \overline{u}}{\partial \overline{t}} + \overline{u} \frac{\partial \overline{u}}{\partial \overline{r}} + \overline{w} \frac{\partial \overline{u}}{\partial \overline{z}} = -\frac{1}{\rho} \frac{\partial \overline{P}}{\partial \overline{r}} + \upsilon \left(\frac{\partial^2 \overline{u}}{\partial \overline{r}^2} + \frac{\partial^2 \overline{u}}{\partial \overline{z}^2} + \frac{1}{\overline{r}} \frac{\partial \overline{u}}{\partial \overline{r}} - \frac{\overline{u}}{\overline{r}^2} \right), \tag{7}$$

$$\frac{\partial \overline{w}}{\partial \overline{t}} + \overline{u} \frac{\partial \overline{w}}{\partial \overline{r}} + \overline{w} \frac{\partial \overline{w}}{\partial \overline{z}} = -\frac{1}{\rho} \frac{\partial \overline{P}}{\partial \overline{z}} + \upsilon \left(\frac{\partial^2 \overline{w}}{\partial \overline{r}^2} + \frac{\partial^2 \overline{w}}{\partial \overline{z}^2} + \frac{1}{\overline{r}} \frac{\partial \overline{w}}{\partial \overline{r}} \right), \tag{8}$$

$$\begin{aligned} \frac{\partial T}{\partial \overline{t}} + \overline{u} \frac{\partial T}{\partial \overline{r}} + \overline{w} \frac{\partial T}{\partial \overline{z}} &= \alpha \left(\frac{\partial^2 T}{\partial \overline{r}^2} + \frac{1}{\overline{r}} \frac{\partial T}{\partial \overline{r}} + \frac{\partial^2 T}{\partial \overline{z}^2} \right) \\ &+ \tau \left[D_B \left(\frac{\partial T}{\partial \overline{r}} \frac{\partial C}{\partial \overline{r}} + \frac{\partial T}{\partial \overline{z}} \frac{\partial C}{\partial \overline{z}} \right) + \frac{D_T}{T_\infty} \left[\left(\frac{\partial T}{\partial \overline{r}} \right)^2 + \left(\frac{\partial T}{\partial \overline{z}} \right)^2 \right] \right], \end{aligned} \tag{9}$$

$$\frac{\partial C}{\partial \bar{t}} + \bar{u}\frac{\partial C}{\partial \bar{r}} + \bar{w}\frac{\partial C}{\partial \bar{z}} = D_B\left(\frac{\partial^2 C}{\partial \bar{r}^2} + \frac{1}{\bar{r}}\frac{\partial C}{\partial \bar{r}} + \frac{\partial^2 C}{\partial \bar{z}^2}\right) + \frac{D_T}{T_\infty}\left(\frac{\partial^2 T}{\partial \bar{r}^2} + \frac{1}{\bar{r}}\frac{\partial T}{\partial \bar{r}} + \frac{\partial^2 T}{\partial \bar{z}^2}\right), \tag{10}$$

$$\frac{\partial n}{\partial \bar{t}} + \bar{u}\frac{\partial n}{\partial \bar{r}} + \bar{w}\frac{\partial n}{\partial \bar{z}} + \frac{\tilde{b}W_c}{C_\infty}\left[\frac{\partial}{\partial \bar{r}}\left(n\frac{\partial C}{\partial \bar{r}}\right) + \frac{\partial}{\partial \bar{z}}\left(n\frac{\partial C}{\partial \bar{z}}\right)\right] = D_n\left(\frac{\partial^2 n}{\partial \bar{r}^2} + \frac{1}{\bar{r}}\frac{\partial n}{\partial \bar{r}} + \frac{\partial^2 n}{\partial \bar{z}^2}\right). \tag{11}$$

The relevant boundary conditions corresponding to the physical problem may be stipulated following Zaimi et al.[43] as:

$$\begin{aligned} &\bar{u}\left(a\left(\bar{t}\right),\ \bar{z}\ ,\ \bar{t}\right) = 0,\ \bar{w}\left(a\left(\bar{t}\right),\ \bar{z}\ ,\ \bar{t}\right) = \frac{4\,\upsilon\,\bar{z}}{a_0^2\left(1-\beta\bar{t}\right)} + N_1\,\upsilon\,\frac{\partial \bar{w}}{\partial \bar{r}},\\ &T = T_w + D_1\frac{\partial T}{\partial \bar{r}},\ D_B\frac{\partial C}{\partial \bar{r}} + \frac{D_T}{T_\infty}\frac{\partial T}{\partial \bar{r}} = 0\,,\ n = n_w \ \text{ at } \ \bar{r} = a\left(\bar{t}\right)\\ &\bar{w}\left(\infty,\ z\ ,\ \bar{t}\right) = 0, \quad T \to T_\infty,\ \ C \to C_\infty,\ \ n \to 0 \ \text{ as } \ \bar{r} \to \infty, \end{aligned} \tag{12}$$

where T_w is the constant surface temperature, N_1 is the velocity slip factor, D_1 is the variable thermal slip factor, n_w is the constant surface density of the motile microorganism, and T_∞ and C_∞ denote constant temperature and nanoparticle volume fraction far from the surface of the cylinder, respectively.

III. SIMILARITY TRANSFORMATION OF MATHEMATICAL MODEL

To proceed, we introduce the following transformations: (Zaimi et al.[43], Abbas et al.[44])

$$\begin{aligned} &\eta = \left(\frac{\bar{r}}{a_0}\right)^2\frac{1}{1-\beta\bar{t}},\quad \bar{u} = -\frac{1}{a_0}\frac{2\,\upsilon}{\sqrt{1-\beta\bar{t}}}\frac{f(\eta)}{\sqrt{\eta}}\,,\quad \bar{w} = \frac{4\,\upsilon\,\bar{z}}{a_0^2\left(1-\beta\bar{t}\right)}f'(\eta)\,,\\ &\theta(\eta) = \frac{T-T_\infty}{T_w-T_\infty},\quad \phi(\eta) = \frac{C-C_\infty}{C_\infty},\quad \chi(\eta) = \frac{n}{n_w}. \end{aligned} \tag{13}$$

Eqn. (6) is satisfies automatically and since there is no longitudinal pressure gradient, Using (13), we have transformed Eqs. (8)-(11) into a system of ordinary differential equations:

$$\eta\,f''' + f'' + f\,f'' - (f')^2 - S\left(\eta\,f'' + f'\right) = 0 \tag{14}$$

$$\eta\theta'' + \theta' + \mathrm{Pr}\,f\,\theta' - \mathrm{Pr}\,S\,\eta\,\theta' + \eta\left[Nb\,\phi'\theta' + Nt\,(\theta')^2\right] = 0, \tag{15}$$

$$Nb\,\eta\,\phi'' + Nb\,\phi' + Sc\,Nb\,(f\,\phi' - S\,\eta\,\phi') + Nt\,(\eta\,\theta'' + \theta') = 0, \tag{16}$$

$$\eta\,\chi'' + \chi' + Sb\,(f\,\chi' - S\,\eta\,\chi') - Pe\left(\eta\,\chi\,\phi'' + \frac{\chi\,\phi'}{2} + \eta\,\phi'\,\chi'\right) = 0. \tag{17}$$

The boundary conditions (13) are transformed into**:**

$$\begin{aligned} &f(1) = 0,\ f'(1) = 1 + b\,f''(1)\ \ ,\ \theta(1) = 1 + c\,\theta'(1),\\ &Nb\,\phi'(1) + Nt\,\theta'(1) = 0\ ,\ \chi(1) = 1,\\ &f'(\infty) = 0\,,\ \theta(\infty) = \ \phi(\infty) = \ \chi(\infty) = 0. \end{aligned} \tag{18}$$

Here, the controlling parameters involved in the above dimensionless Eqs. (14)-(18) are $S = \frac{a_0^2\beta}{4\,\upsilon}$ is the unsteadiness parameter, $\mathrm{Pr} = \frac{\upsilon}{\alpha}$ is the Prandtl number, $Nb = \frac{\tau D_B C_\infty}{\alpha}$ is the Brownian motion parameter, $Nt = \frac{\tau D_T(T_w - T_\infty)}{\alpha T_\infty}$ is the thermophoresis parameter, $Sc = \frac{\upsilon}{D_B}$ is the Schmidt number, $Sb = \frac{\upsilon}{D_n}$ is the bioconvection Schmidt number, $Pe = \frac{\tilde{b}W_c}{D_n}$ is the Péclet number, $b = \frac{2\,(N_1)_0\upsilon}{a_0}$ is the velocity slip parameter, $c = \frac{2(D_1)_0}{a_0}$ is the thermal slip parameter . The pressure can be obtained from Eq. (7) as

$$\frac{P}{\rho} = \text{constant} + \upsilon\left(\frac{\partial \bar{u}}{\partial \bar{r}} + \frac{\bar{u}}{\bar{r}}\right) - \frac{1}{2}\bar{u}^2 + \int\frac{\partial \bar{u}}{\partial \bar{t}}\,\partial\bar{t}. \tag{19}$$

IV. PHYSICAL QUANTITIES

The quantities of engineering interest in bio-nano-materials processing are the wall parameters. These are respectively local skin friction coefficient $C_{f_{\bar{x}}}$, local Nusselt number $Nu_{\bar{x}}$, local nano-particle mass transfer rate i.e. local Sherwood number, and finally the local density number of motile micro-organisms, $Nn_{\bar{x}}$ defined as:

$$C_{f_{\bar{x}}} = \frac{\tau_w}{\rho \overline{w}_w^2/2}, Nu_{\bar{x}} = \frac{\overline{a}\,(\bar{t})\, q_w}{2k(T_w - T_\infty)}, Sh_{\bar{x}} = \frac{\overline{a}\,(\bar{t})\, q_m}{2D_B(C_w - C_\infty)}, Nn_{\bar{x}} = \frac{\overline{a}\,(\bar{t})\, q_n}{2kn_w}, \tag{20}$$

where τ_w, q_w, q_m and q_n represent the *shear stress, surface heat flux, surface mass flux* and *the surface motile microorganism flux* and are defined by:

$$\tau_w = \mu \left.\frac{\partial \overline{w}}{\partial \overline{r}}\right|_{\overline{r}=a(\bar{t})}, q_w = -k \left.\frac{\partial T}{\partial \overline{r}}\right|_{\overline{r}=a(\bar{t})}, q_m = -D_B \left.\frac{\partial C}{\partial \overline{r}}\right|_{\overline{r}=a(\bar{t})}, q_n = -D_n \left.\frac{\partial n}{\partial \overline{r}}\right|_{\overline{r}=a(\bar{t})}. \tag{21}$$

Substitute Eqns. (21) and (13) into (20) we obtain:

$$C_{f_{\bar{x}}} z/\overline{a}\,(\bar{t}) = f''(1), Nu_{\bar{x}} = -\theta'(1), Sh_{\bar{x}} = \frac{-\phi'(1)}{\phi(1)}, Nn_{\bar{x}} = -\chi'(1). \tag{22}$$

V. MAPLE 18 NUMERICAL SOLUTION, SPECIAL CASES AND VALIDATION

Numerical solutions to the ordinary differential Eq. (14) – (17) subject to the boundary conditions (18) were obtained using Runge-Kutta-Felhbergh fourth-fifth order quadrature (shooting methods) in the Maple software via built-in functions. This approach has been successfully used by many researchers in order to solve high order systems of coupled, nonlinear ordinary differential equations (ODEs). Readers are referred for example to Uddin et al.,[45] Khan et al.[46] When Eqns. (15) – (17) are removed the present generalized unsteady forced bioconvection nanofluid dynamic model reduces to the model studied by Fang et al.[47] and also setting $Re = 1$ we retrieve the model of Fang et al.[41] Furthermore for $S = 0$ (steady case), $Nt = Nb = 0$ (nano-particle absence) and disregarding Eqns. (16) and (17), the general model developed in eqns. (14)-(18) reduces to the case examined by Ishak et al.[48] when $M = 0$ and Re = 1 is prescribed in their paper. Finally the model studied by Zaimi et al.[49] is retrieved exactly when Eqns. (16) and (17) are neglected and $Nt = Nb = 0$ is prescribed in the general model defined by eqns. (14) to (18). To validate the accuracy of our present code, we compare the numerical result for the local skin friction coefficient $f''(1)$ and $-\theta'(1)$ when $S = 0$, $M = 0$ and $Re = 1$ with the solutions given by Ishak et al.[48] and Wang.[50] In real situations, minus sign of $f''(1)$ infers that the stretching cylinder/tube applies dragging force on the fluid flow and vice versa (Ishak et al.[48]). Solutions obtained via MAPLE 18 are benchmarked with these previous studies and in all cases excellent agreement is obtained. All comparison tables are documented in the Appendix (see Tables I and II). There is therefore justifiably high confidence in the present MAPLE18 solutions.

VI. NUMERICAL RESULTS AND DISCUSSION

In this section, we present the effects of parameters b, c, S and Sb on $f'(\eta)$, $\theta(\eta)$, $\phi(\eta)$ and $\chi(\eta)$. All computations illustrated in the figs. 2-6 were performed using MAPLE18 software We fix the value of Pr, Nb, Nt, Sc, Pe corresponding to Kuznetsov and Nield.[51] The effects of these parameters are well-established and are therefore not re-visited here. We focus principally on the influence of unsteadiness (S), hydrodynamic wall slip (b), thermal slip (c) and bioconvection Schmidt number (Sb).

Figs. 2(a)–2(d) shows the variations in dimensionless velocity, temperature, nanoparticle volume fraction and motile microorganism density function, respectively for different values of unsteadiness parameter (S) and velocity slip (b) for the stretching cylinder scenario. It is necessary to point out that the value of positive S indicates *accelerating flow* and negative S corresponds to *decelerating flow*

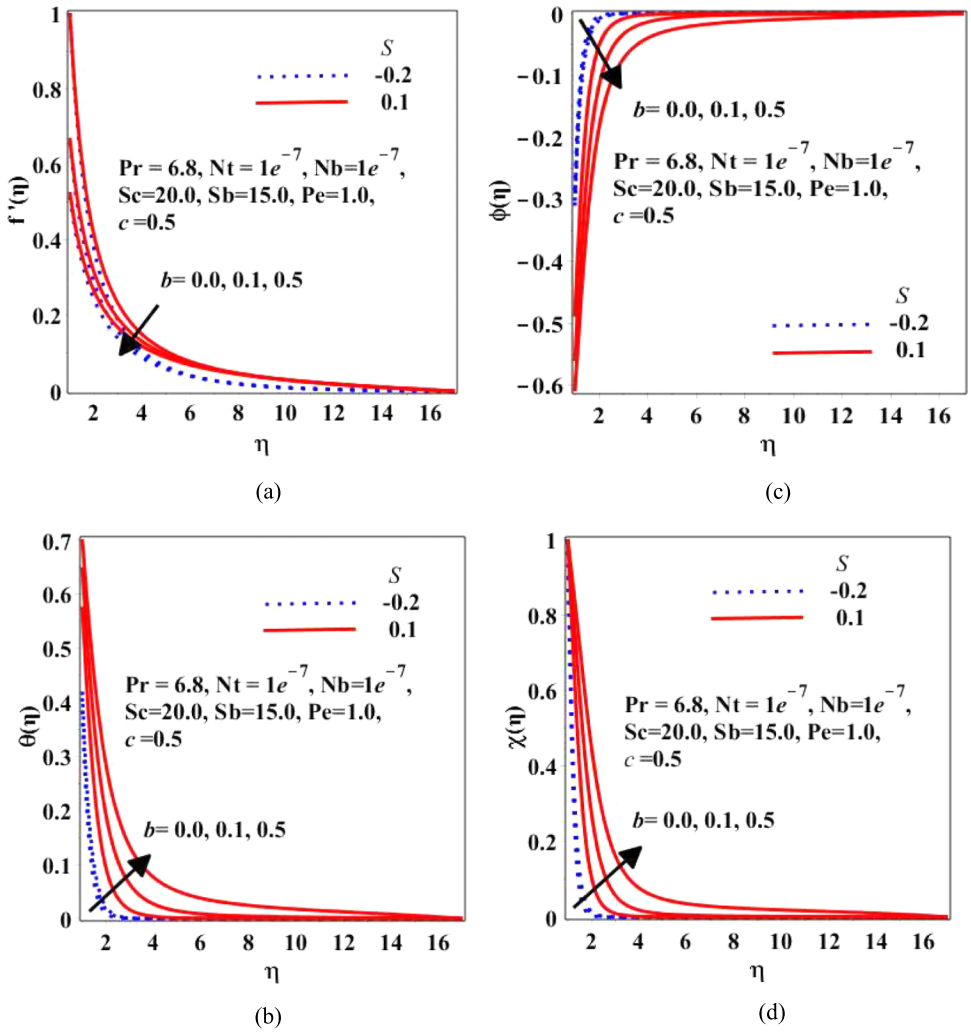

FIG. 2. Effect of unsteadiness (S) and velocity slip (b) on the (a) velocity (b) temperature, (c) nanoparticle volume fraction, (d) motile microorganism density profiles.

of the surface of the cylinder, which is being stretched. Therefore for $S \neq 0$ the flow is *unsteady* and for $S = 0$ it is *steady*. From Fig. 2(a), the dimensionless velocity decreases with increasing velocity (hydrodynamic) slip for both positive and negative value of S. When slip ensues, the velocity close to surface stretching wall is not equivalent to the stretching velocity of the wall. Additionally under slip conditions, the dragging of the stretching wall can only be partially transmitted to the fluid and this causes the fluid velocity to fall i.e. induces retardation in the boundary layer flow. These results are consistent with published work by Mukhopadhyay[52] and also Wang.[53] Furthermore, the magnitude of the wall shear stress decreases with an increase in the hydrodynamic slip factor.

The case of $b = 0$ applies to the classical non-slip scenario. The momentum boundary-layer thickness decreases with an increase in the velocity slip parameter. In Fig. 2(b), for both $S>0$ (accelerating cylinder) or $S<0$ (decelerating cylinder), with an increasing the velocity slip, b, the dimensionless temperature, $\theta(\eta)$, is markedly enhanced. However temperatures are somewhat greater for the accelerating cylinder case as compared with the decelerating case. The thermal boundary-layer thickness therefore increases with an increase in the velocity slip parameter. The deceleration in the velocity field, $f^{/}(\eta)$, implies that momentum diffusion is reduced. This benefits the transport of heat via thermal diffusion which manifests in a heating in the bio-nano-boundary layer regime and an associated elevation in temperature. Thermal diffusivity is dominant in this case i.e. heat

conduction is stronger than heat convection. Both velocity and temperature profiles are found to decay smoothly from maxima at the cylinder surface to the free stream, indicating that a sufficiently large infinity boundary condition has been imposed in the MAPLE18 computational domain. The dimensionless nanoparticle volume fraction (nano-particle concentration), ϕ (η), as depicted in Fig. 2(c) is observed to be reduced with increasing velocity slip. The nano-particle concentration boundary-layer thickness will therefore be increased with a rise in the velocity slip parameter. The dimensionless concentration also *decreases for accelerated* flow ($S>0$) whereas it is *elevated for decelerated* ($S<0$) flow. The prescribed Schmidt number in Fig. 2 is 20.0. Schmidt number (Sc) expresses the ratio of momentum diffusivity to species diffusivity i.e. viscous diffusion rate to molecular (nano-particle) diffusion rate. Sc is also the ratio of the shear component for diffusivity *viscosity/density* to the diffusivity for mass transfer D. It physically relates the relative thickness of the hydrodynamic layer and mass-transfer boundary layer. We further note that Pr is prescribed as 6.8 as this quite accurately represents water-based nano-bio-polymers. The deceleration in the flow with increasing hydrodynamic slip also acts to decrease molecular diffusion rate (via the Schmidt number) and this will result in decreasing nano-particle boundary layer thickness. The depletion in nanoparticle concentration will cause a corresponding elevation in nano-particle mass transfer rate at the cylinder surface (wall). From Fig. 2(d), it is evident that the dimensionless microorganism number density function, $\chi(\eta)$ increases as velocity slip increases i.e. with flow *deceleration*. The behavior is different from the nano-particle concentration field. Unlike the diffusion of nano-particles (which is molecular in nature), the micro-organisms move by flagellar propulsion which is encouraged in slower flows. They are therefore able to propel more evenly through the boundary layer for slower flow. The microorganism boundary layer thickness also increases with increasing velocity slip. The implication is that more homogenous distributions of micro-organisms through the boundary layer regime are achieved with deceleration in the flow. This is desirable in the manufacture of biodegradable nano-polymers as further elaborated by Thomas and Yang.[3] It is also observed that $\chi(\eta)$ values are greater for the accelerating cylinder case ($S>0$) as compared with the decelerating cylinder case ($S<0$). Therefore contrary responses in the micro-organism number density magnitudes are induced depending on whether the *boundary layer flow* is accelerating (which it does for no-slip) or the *cylinder* is accelerating. The former is associated with slip absence (or presence which causes deceleration in the flow) whereas the latter is connected to the unsteadiness in the cylinder stretching motion.

Figure 3(a)–3(c) display the collective influence of thermal slip parameter (c) and unsteadiness parameter (S) on dimensionless temperature, concentration and microorganism profiles respectively. It is apparent that the thermal slip parameter leads to a decline in dimensionless temperature (Fig. 3(a)). The greatest effect is as expected at the cylinder surface. Physically, as the thermal slip parameter rises, the fluid flow within the boundary layer will be less sensitive to the heating effects of the cylinder surface and a reduced quantity of thermal energy (heat) will be transmitted from the hot cylinder to the fluid, resulting in a fall in temperatures i.e. cooling and thinning of the thermal boundary layer (decrease in thermal boundary layer thickness). For an accelerating stretching cylinder ($S>0$), the temperatures are substantially higher than for a decelerating stretching cylinder ($S<0$). The dimensionless nano-particle concentration is found to be strongly increased with greater thermal slip. Nano-particle concentration however is enhanced for the decelerating stretching cylinder case whereas it is depressed for the accelerating cylinder case. Micro-organism number density function (Fig 3(c)) is however significantly decreased with increasing thermal slip effect. For an accelerating stretching cylinder ($S>0$), the micro-organism density is (as with temperature) unlike nano-particle concentration, substantially higher than for a decelerating stretching cylinder ($S<0$). Micro-organism number density and temperature profiles are very similar indicating that fields respond in a similar fashion in the external boundary layer regime on the stretching cylinder. Thermal diffusion and micro-organism propulsion obey similar physics in the flow as opposed to nano-particle diffusion which has a distinctly different response. An increase in thermal slip essentially thickens both the thermal and micro-organism number density boundary layers whereas it thins the nano-particle concentration boundary layer thickness. Therefore biotechnological engineers can achieve very different thermo-fluid characteristics in nano-bio-polymers by

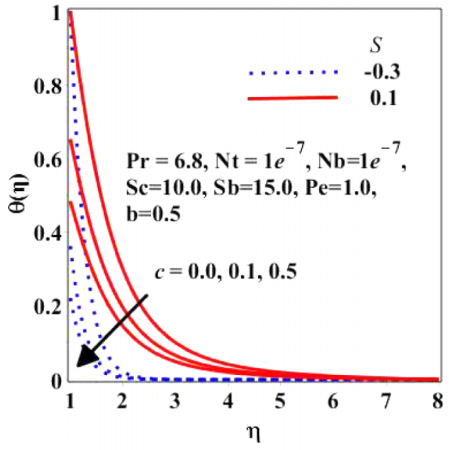

(a)

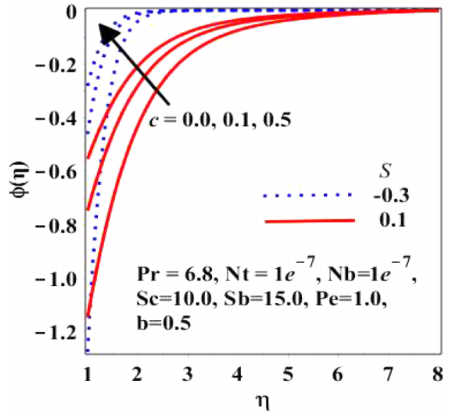

(b)

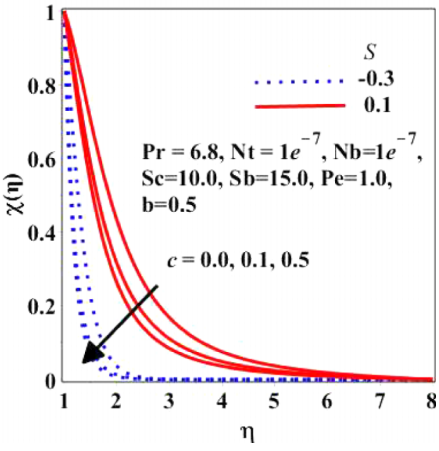

(c)

FIG. 3. Effect of unsteadiness (S) and thermal slip (c) on the dimensionless temperature, (b) nanoparticle volume fraction and (c) microorganism density profiles.

judiciously utilizing thermal slip at the cylinder wall and also via the rate of cylinder stretching (unsteadiness).

Fig. 4 illustrates the response of micro-organism number density to a variation in bioconvection Schmidt number, Sb. This parameter features solely in the micro-organism density conservation

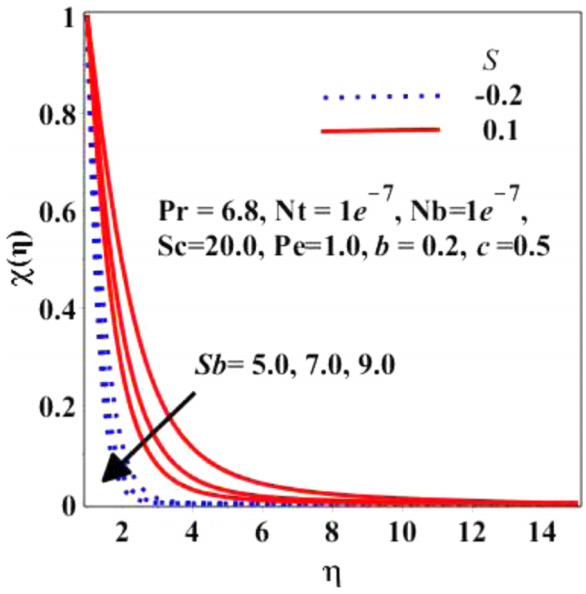

FIG. 4. Effect of unsteadiness (S) and bioconvection Schmidt number (Sb) on the dimensionless motile microorganism density function.

eqn. (17), in a similar way to the conventional Schmidt number (Sc) arises only in the nano-particle species conservation eqn. (16). It is defined as $Sb = \frac{\upsilon}{D_n}$, in other words the ratio of momentum diffusivity to diffusivity of microorganisms. For $Sb > 1$ as studied in Fig. 4, momentum diffusivity exceeds micro-organism diffusivity. As this parameter increases the difference in diffusivity is amplified and momentum diffusion rate increasingly dominates the micro-organism diffusion rate leading to a reduction in micro-organism density number magnitudes, $\chi(\eta)$. There is a corresponding diminishing in the thickness of the micro-organism number density boundary layer. For an accelerating stretching cylinder ($S>0$), the micro-organism density is significantly higher than for a decelerating stretching cylinder ($S<0$).

Figs. 5 and 6 depict the variation of selected parameters on the heat transfer rate $-\theta'(1)$ and motile micro-organism number transfer rate, $-\chi'(1)$ are illustrated in. Figure 5 shows the variations

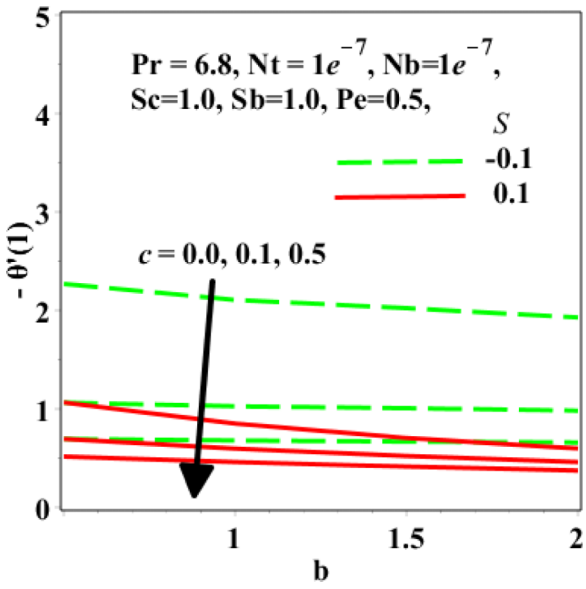

FIG. 5. Effect of velocity slip (b) and thermal slip (c) parameters on the wall heat transfer rate.

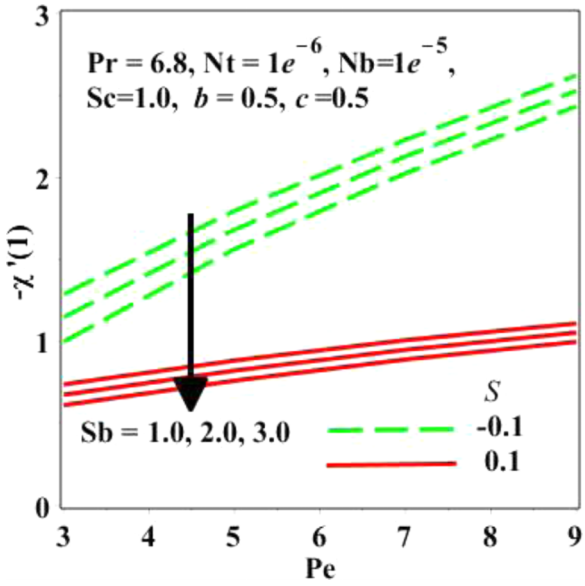

FIG. 6. Effect of bioconvection Schmidt number (S*b*) and bioconvection Péclet number (*Pe*) parameters on the microorganism density wall transfer rate.

of $-\theta'(1)$ versus c and S for different values of b. It is found that $-\theta'(1)$ decreases strongly with increasing thermal slip (c) and relatively weakly with increasing hydrodynamic slip (b). For an accelerating stretching cylinder ($S>0$), motile micro-organism number transfer rate is substantially reduced whereas it is significantly enhanced for the decelerating stretching cylinder ($S<0$) case. Figure 6 shows the effects of S, Sb and Pe on $-\chi'(1)$. $-\chi'(1)$ is found to be increased with bioconvection Péclet number (Pe). Pe is directly proportional to $\tilde{b}$ (chemotaxis constant) and W_c (maximum cell swimming speed) and inversely proportional to D_n (diffusivity of microorganisms). Therefore for higher Pe values the micro-organism speed will be reduced and/or the diffusivity of micro-organisms will be decreased. This will result in reduced concentrations of micro-organisms in the boundary layer and an elevation in motile micro-organism mass transfer rate, $-\chi'(1)$, to the cylinder surface, as observed in Figure 6. $-\chi'(1)$ is also observed to be decreased for a decelerating cylinder ($S<0$) and increased for an accelerating cylinder ($S>0$). With increasing bioconvection Schmidt number there is a substantial depression in motile micro-organism mass transfer rate, $-\chi'(1)$. We further note that since no tangible variations are computed in nano-particle mass transfer rate $\frac{-\phi'(1)}{\phi(1)}$ and local skin friction factor $-f''(1)$ with bioconvection Schmidt or biconvection Péclet number, these distributions have been omitted.

VII. CONCLUSIONS

The unsteady bioconvective slip flow of a nanofluid (containing both nanoparticles and gyrotactic microorganisms) in the external boundary layer from a stretching cylinder, is studied as a simulation of bio-nano-polymer fabrication. The Buongiorno nanofluid model is employed with physically more realistic passively controlled boundary conditions. Both thermal and hydrodynamic slip effects at the cylinder surface are considered. The governing transport equations are transformed into a set of ordinary differential equations using similarity variables. The transformed well-posed ninth order boundary value problem is solved using the Runge–Kutta-Felhberg fourth-fifth order numerical method in MAPLE18 symbolic software. Validation with previous computations is included. The computations have shown that increasing bioconvection Schmidt number reduces motile micro-organism density function. Increasing hydrodynamic slip enhances temperatures and motile micro-organism density function, but decreases nanoparticle volume fraction (nano-particle concentration) values. Increasing thermal slip reduces temperatures and furthermore

for an accelerating stretching cylinder ($S>0$), the temperatures are greater than for a decelerating stretching cylinder ($S<0$). Nano-particle concentration is conversely elevated with greater thermal slip whereas micro-organism number density function is greatly depressed with increasing thermal slip effect. At any bioconvection Schmidt number, for an accelerating stretching cylinder ($S>0$), the micro-organism density is much higher than for a decelerating stretching cylinder ($S<0$). Local Nusselt number is reduced with increasing hydrodynamic and thermal slip and also for an accelerating cylinder. The local microorganism transfer rate is increased with greater values of bioconvection Péclet number whereas it is suppressed with greater bioconvection Schmidt number and for an accelerating cylinder (positive values of unsteadiness parameter). The present work has been confined to constant fluid properties and ignored electromagnetic effects. For future work, the present model may therefore be extended to consider variable fluid properties and also multi-physical effects e.g. chemical reaction, magnetohydrodynamics, second order slip and melting effects. These are also relevant to bio-nano-polymer processing applications and efforts in this regard are under way.

ACKNOWLEDGEMENTS

The authors acknowledge financial support from Universiti Sains Malaysia, RU Grant 1001/PMATHS/81125. All the authors are grateful to the reviewer for his/her comments which have served to improve the present article.

APPENDIX: VALIDATION TABLES

TABLE I. Values of the skin friction factor $f''(1)$ for $\mathrm{Pr} = 0.7$.

	Ishak et al.[48]	Wang[50]	Present Study
$f''(1)$	-1.1780	-1.17776	-1.17805

TABLE II. Values of the Nusselt number $-\theta'(1)$ for $\mathrm{Pr} = 7$.

	Ishak et al.[48]	Wang[50]	Present Study
$-\theta'(1)$	2.0587	2.059	2.05862

[1] N. Bachok and A. Ishak, "Flow and heat transfer over a stretching cylinder with prescribed surface heat flux," Malaysian Journal of Mathematical Sciences **4**, 159–169 (2010).
[2] J. Stasiak, A. M. Squires, V. Castelletto, I. W. Hamley, and G. D. Moggridge, "Effect of stretching on the structure of cylinder- and sphere-forming Styrene-Isoprene-Styrene block copolymers," Macromolecules **42**, 5256–5265 (2009).
[3] S. Thomas and W. Yang (eds.), *Advances in Polymer Processing: From Macro- To Nano-Scales* (Elsevier, USA, 2009).
[4] W.A. Khan and I. Pop, "Boundary-layer flow of a nanofluid past a stretching sheet," Int. J. Heat Mass transf. **53**(11–12), 2477-2483 (2010).
[5] M. K. Partha, P.V.S.N. Murthy, and G.P. Rajasekhar, "Effect of viscous dissipation on the mixed convection heat transfer from an exponentially stretching surface," Heat and Mass Transf **41**, 360-366 (2005).
[6] A. Ishak, R. Nazar, and I. Pop, "Mixed convection on the stagnation point flow toward a vertical, continuously stretching sheet," ASME J. Heat Transf **129**, 1087–1090 (2007).
[7] O. A. Bég, A. Y. Bakier, and V. R. Prasad, "Numerical study of free convection magnetohydrodynamic heat and mass transfer from a stretching surface to a saturated porous medium with Soret and Dufour effects," Computational Materials Sci **46**, 57-65 (2009).
[8] J. E. Daskalakis, "Free Convection effects in the boundary layer along a vertically stretching flat surface," Canadian J. Phy **70**, 1253 (1993).
[9] M. Y. Akl, "Unsteady boundary layer flow along a stretching cylinder an analytical solution," J. Mathematics and Statistics **10**, 117 (2014).

[10] O. A. Bég, U. S. Mahabaleshwar, M. M. Rashidi, N. Rahimzadeh, J-L Curiel Sosa, Ioannis Sarris, and N. Laraqi, "Homotopy analysis of magneto-hydrodynamic convection flow in manufacture of a viscoelastic fabric for space applications," Int. J. Appl. Maths. Mech **10**, 9-49 (2014).
[11] S. U S. and Choi, "Enhancing thermal conductivity of fluids with nanoparticles," in *Proc. 1995 ASME International Mechanical Engineering Congress and Exposition*, *San Francisco, USA, ASME, FED 231/MD* (1995), Vol. 66, pp. 99–105.
[12] Y. Li, S. Tung, E. Schneider, and S. Xi, "A review on development of nanofluid preparation and characterization," Powder Tech **196**, 89-101 (2009).
[13] J. Buongiorno, "Convective transport in nanofluids," ASME J. Heat Transf **128**, 240–250 (2006).
[14] S. K. Das, S. U. Choi, W. Yu, and T. Pradeep, *Nanofluids: Science and Technology* (John Wiley and Sons, 2007).
[15] S. Kakac and A. Pramuanjaroenkij, "Review of convective heat transfer enhancement with nanofluids," Int. J. Heat and Mass Transf **52**, 3187-3196 (2009).
[16] R. Saidur, K. Y. Leong, and H. A. Mohammad, "A review on applications and challenges of nanofluids," Renew. and Sus. Energy Rev **15**, 1646-1668 (2011).
[17] D. Wen, G. Lin, S. Vafaei, and K. Zhang, "Review of nanofluids for heat transfer applications," Particuology. **7**, 141-150 (2009).
[18] O. Mahian, A. Kianifar, S. A., Kalogirou, I. Pop, and S. Wongwises, "A review of the applications of nanofluids in solar energy," Int. J. Heat and Mass Transf **57**, 582-594 (2013).
[19] D. A. Nield and A. Bejan, *Convection in Porous Media (fourth ed.)* (Springer, New York, 2013), pp. 582–594.
[20] Z. Haddad, E. Abu-Nada, and A. Mataoui, "Natural convection in nanofluids: are the thermophoresis and Brownian motion effects significant in nanofluid heat transfer enhancement," Int. J. Therm. Sci **57**, 152–162 (2012).
[21] M. A. Sheremet and I. Pop, "Free convection in a porous horizontal cylindrical annulus with a nanofluid using Buongiorno's model," Computers & Fluids **118**, 182-190 (2015).
[22] R. K. Tiwari and M. K. Das, "Heat transfer augmentation in a two-sided lid-driven differentially heated square cavity utilizing nanofluids," Int. J. Heat and Mass Transf **50**, 2002-2018 (2007).
[23] M. Ghanbarpour, N. Nikkam, R. Khodabandeh, and M. S. Toprak, "Improvement of heat transfer characteristics of cylindrical heat pipe by using sic nanofluids," Appl. Therm. Eng **90**, 127–135 (2015).
[24] H. Li, Y. He, Y. Hu, B. Jiang, and Y. Huang, "Thermophysical and natural convection characteristics of ethylene glycol and water mixture based Zno nanofluids," Int. J. Heat and Mass Transf **91**, 385–389 (2015).
[25] S. M. Vanaki, P. Ganesan, and H. A. Mohammed, "Numerical study of convective heat transfer of nanofluids: A review," Renew. and Sus. Ener. Rev **54**, 1212-1239 (2016).
[26] N. Zhao, J. Yang, H. Li, Z. Zhang, and S. Li, "Numerical investigations of laminar heat transfer and flow performance of Al 2 O 3–water nanofluids in a flat tube," Int. J. Heat and Mass Transf. **92**, 268-282 (2016).
[27] J. Serna, "Heat and mass transfer mechanisms in nanofluids boundary layers," Int. J. Heat and Mass Transf **92**, 173-183 (2016).
[28] S. T. Mohyud-Din, Z. A. Zaidi, U. Khan, and N. Ahmed, "On heat and mass transfer analysis for the flow of a nanofluid between rotating parallel plates," Aerospace Sci. and Tech. **46**, 514-522 (2015).
[29] M. Ferdows, M. S. Khan, O. A. Bég, M. A. K. Azad, and M. M Alam, "Numerical study of transient magnetohydrodynamic radiative free convection nanofluid flow from a stretching permeable surface," Proc. IMechE-Part E, J. Process Mech. Eng **228**, 181-196 (2014).
[30] M. J. Uddin, O. A. Bég, N. Amran, and A. I. MD. Ismail, "Lie group analysis and numerical solutions for magneto-convective slip flow of a nanofluid over a moving plate with a Newtonian heating boundary condition," Can. J. Phys **93**, 1–10 (2015).
[31] A. V. Kuznetsov, "Nanofluid bioconvection in water-based suspensions containing nanoparticles and oxytactic microorganisms: Oscillatory instability," Nanoscale Res. Lett **6**, 100 (2011).
[32] A. Raees, H. Xu, and S. J. Liao, "Unsteady mixed nano-bioconvection flow in a horizontal channel with its upper plate expanding or contracting," Int. J. Heat and Mass Transf **86**, 174-182 (2015).
[33] K. B. Anoop, T. Sundararajan, and S. K. Das, "Effect of particle size on the convective heat transfer in nanofluid in the developing region," Int. J. Heat and Mass Transf **52**, 2189–2195 (2009).
[34] T. J. Pedley, "Instability of uniform micro-organism suspensions revisited," J. Fluid Mechanics. **647**, 335-359 (2010).
[35] H. Xu and I. Pop, "Mixed convection flow of a nanofluid over a stretching surface with uniform free stream in the presence of both nanoparticles and gyrotactic microorganisms," Int. J. Heat and Mass Transf **75**, 610-623 (2014).
[36] A. Aziz, W. A. Khan, and I. Pop, "Free convection boundary layer flow past a horizontal flat plate embedded in porous medium filled by nanofluid containing gyrotactic microorganisms," Int. J. Therm. Sci **56**, 48–57 (2012).
[37] N. A. A., Latiff, M.J. Uddin, O.A., Bég, and A.I.M. Ismail, "Unsteady forced bioconvection slip flow of a micropolar nanofluid from a stretching/shrinking sheet," Proc. IMECHE-Part N: J. of Nano. and Nanosys. 1740349915613817 (2015).
[38] L. Tham, R. Nazar, and I. Pop, "Mixed convection flow over a solid sphere embedded in a porous medium filled by a nanofluid containing gyrotactic microorganisms," Int. J. Heat and Mass Transf. **62**, 647-660 (2013).
[39] S. Saranya and K. V. Radha, "Review of nanobiopolymers for controlled drug delivery," Polymer-Plastics Tech. and Eng. **53**, 1636-1646 (2014).
[40] J. K. Oh, D. I. Lee, and J. M Park, "Biopolymer-based microgels/nanogels for drug delivery applications," Progress in Polymer Sci **34**, 1261-1282 (2009).
[41] T. Fang, J. Zhang, and Y. Zhong, "Unsteady viscous flow over an expanding stretching cylinder," Chinese Phys. Lett **28**, 124707 (2011).
[42] A. V. Kuznetsov and D. A. Nield, "Natural convective boundary-layer flow of a nanofluid past a vertical plate: A revised model," Int. J. Therm. Sci **77**, 126-129 (2014).
[43] K. Zaimi, A. Ishak, and I. Pop, "Unsteady flow due to a contracting cylinder in a nanofluid using Buongiorno's model," Int. J. Heat and Mass Transf **68**, 509-513 (2014).
[44] Z. Abbas, M. Sheikh, and I. Pop, "Stagnation-point flow of a hydromagnetic viscous fluid over stretching/shrinking sheet with generalized slip condition in the presence of homogeneous–heterogeneous reactions," J. Taiwan Inst. Chem. Eng **55**, 69-75 (2015).

[45] M. J. Uddin, O. A. Bég, and A. I. Ismail, "Radiative convective nanofluid flow past a stretching/shrinking sheet with slip effects," AIAA J. Thermophysics and Heat Transf 1-11 (2015).
[46] W. A. Khan, O. D. Makinde, and Z. H. Khan, "MHD boundary layer flow of a nanofluid containing gyrotactic microorganisms past a vertical plate with Navier slip," Int. J. Heat and Mass Transf. **74**, 285-291 (2014).
[47] T. Fang, J. Zhang, and Y. Zhong, "Note on unsteady viscous flow on the outside of an expanding or contracting cylinder," Comm. Nonlinear Sci. and Numer. Simulat. **17**, 3124-3128 (2012).
[48] A. Ishak, R. Nazar, and I. Pop, "Magnetohydrodynamic (MHD) flow and heat transfer due to a stretching cylinder," Energy Conver. and Managt **49**, 3265–3269 (2008).
[49] W. W. Zaimi, A. Ishak, and I. Pop, "Unsteady viscous flow over a shrinking cylinder," J. King Saud University-Science. **25**, 143-148 (2013).
[50] C. Y. Wang, "Fluid flow due to a stretching cylinder," Phy. of Fluids **31**, 466-468 (1988).
[51] A. V. Kuznetsov and D. A. Nield, "Natural convective boundary-layer flow of a nanofluid past a vertical plate," Int J Therm Sci **49**, 243–247 (2010).
[52] S. Mukhopadhyay, "MHD boundary layer slip flow along a stretching cylinder," Ain Shams Eng J. **4**, 317–324 (2013).
[53] C. Y. Wang, "Analysis of viscous flow due to a stretching sheet with surface slip and suction," Nonlinear Analysis: Real World Appl. **10**, 375-380 (2009).